Stony Brook University

Sorption Behavior of Antimony(V) on Hydroxyapatite

A Thesis Presented

by

Boyoung Song

to

The Graduate School

in Partial Fulfillment of the

Requirements

for the Degree of

Master of Science

in

Department of Geoscience

Stony Brook University

December 2014

Stony Brook University

The Graduate School

Boyoung Song

We, the thesis committee for the above candidate for the

Master of Science degree, hereby recommend

acceptance of this thesis.

Richard J. Reeder – Thesis Advisor
Professor
Department of Geoscience

Brian L. Phillips – Chair
Professor
Department of Geoscience

Gilbert N. Hanson
Distinguished Professor
Department of Geoscience

This thesis is accepted by the Graduate School

Charles Taber
Dean of the Graduate School

Abstract of the Thesis

Sorption Behavior of Antimony(V) on Hydroxyapatite

by

Boyoung Song

Master of Science

in

Department of Geoscience

Stony Brook University

2014

Antimony (Sb) is regarded as an emerging environmental contaminant, reflecting its previously unrecognized presence in aquatic and soil systems. Oxidative dissolution releases Sb into surface environments primarily in the form of oxyanions. A primary control on the mobility of Sb species is sorption onto mineral surfaces. Although recent studies have reported Sb sorption onto various mineral surfaces, no studies have been performed on the sorption behavior of Sb with hydroxyapatite, which is an effective sorbent. The objective of this study is to understand the sorption behavior of Sb(V) on the surface of hydroxyapatite, $Ca_5(PO_4)_3OH$. The oxidized form of antimony, Sb(V), occurs mainly as $Sb(OH)_6^-$ in aqueous systems above pH 3.

In the present study, batch sorption experiments were conducted over a range of conditions, including pH, ionic strength, and initial concentration of Sb(V). All sorption experiments were conducted in solution that was pre-equilibrated with hydroxyapatite, using a particle loading of 1.0 gL^{-1}. The range of solution conditions encompassed pH 5.5-8.0, ionic strength 0.005 and 0.01 M, and initial Sb(V) concentration from 50-2000 μM. The isotherm experiments (determined at 24 hr) showed that Sb(V) sorption decreases

as pH increases at I = 0.005 M. However, a sharp increase in uptake in the isotherm suggests that precipitation occurred in the solution at [Sb(V)] > 1000 μM. The type of background electrolyte has an effect on the sorption behavior of Sb(V). Using NaCl as the background electrolyte, evidence for the onset of precipitation was found at a lower Sb(V) concentration at I = 0.01 M (compared to I = 0.005 M), and was more pronounced at pH 7.0 and 8.0. To confirm formation of a solid precipitate in the solution, the filtered, dried samples were analyzed with powder X-ray diffraction. Sodium hexahydroantimonate ($NaSb(OH)_6$), with the mineral name mopungite, was observed as the only secondary phase. Above the initial Sb(V) concentration 1000 μM, mopungite formed over the entire pH range at I = 0.005 M, and was observed to form at lower Sb(V) concentration at I = 0.01 M. This precipitation dominates sorption behavior of Sb(V) on hydroxyapatite at higher Sb concentrations.

This study suggests that lower concentrations of Sb(V) could be effectively removed by sorption on hydroxyapatite at I = 0.005 M, consistent with previous work showing that metal oxides are effective sorbents of Sb(V). However, the sorption behavior of Sb(V) is critically affected by the existence of Na^+ in the solution, which may promote precipitation. In nature, Na^+ is one of the most abundant ions in aquatic systems, especially freshwater and seawater. Therefore, a comprehensive understanding of actual conditions, including properties of the aqueous and solid phases, is necessary for predicting the transport and fate of Sb in the environment.

Table of Contents

List of Figures

Figure 13. Use of non linear regression for the Langmuir and Freundlich models (pH 5.5, I = 0.005 M, pH 8.0, I = 0.01 M)

List of Tables

Acknowledgments

I sincerely thank to my advisor, Dr. Richard J. Reeder for his support, guidance and encouragement in finishing my research. I respect you with all my heart and am appreciated to you for giving me an opportunity to work with you.

I also thank to my friends, Haeyeong Ryu and Songhwa Choi who spent most of my graduate life together with their support.

Most of all, I am specially appreciated to my parents and my younger brother, Ki-eun, for supporting my with all their heart. I cannot express how grateful I am for the sacrifices you made for me. Thank you for everything as always. Love with all my heart.

INTRODUCTION

Antimony (Sb) is regarded as an emerging environmental contaminant in aquatic and soil systems. Antimony naturally occurs in soils and rocks at very low concentrations (e.g., 1 µg/L) in non-polluted waters. The maximum contaminant level (MCL) is 6 µg/L for drinking water (United States Environmental Protection Agency). However, high Sb concentrations can be found at contaminated sites associated with mining, ore deposits and widespread industrial use such as flame retardants, semiconductors, lead batteries, and lead alloys. As industrial uses for Sb increase, the fate and movement of Sb has become a growing concern (Filella et al., 2002b). Oxidative dissolution of metallic forms releases Sb into surface environments primarily in the form of oxyanions. Sb is classified as a metalloid and belongs to Group 15 in the periodic table, below phosphorus and arsenic. In nature, Sb exists in various oxidation states ranging from -3 to +5. However, Sb(III) and Sb(V) are only the dominant oxidation states for dissolved species in the environment, occurring mainly as the oxyanions $Sb(OH)_3$ and $Sb(OH)_6^-$, respectively (Filella et al. (2002b), Figure 1). In well oxidized surface environments above pH 3, $Sb(OH)_6^-$ is the dominant dissolved species in solution (Figure 2).

Sorption onto solid surfaces commonly constrains the fate and transport of both of inorganic and organic species in natural aquatic settings (Sposito (1984), Jenne (1998), Hem (1977)). For this reason, the sorption process is often applied to remove dissolved contaminants during water treatment or purification in engineered systems. Sorption behavior is influenced by various physical and chemical conditions such as sorbate concentration, pH, redox potential, particulate loading, the presence of competing ions, and properties of the sorbent (Smith, 1999). Hydroxyapatite, $Ca_5(PO_4)_3OH$, is a common mineral constituent in soils, sediments, and forms among all three rock types. Hydroxyapatite (HAP) also exists as a major constituent of bones and teeth of human body in a modified form (Smičiklas et al., 2006). Hydroxyapatite is the most stable calcium phosphate at room temperature and in solution over the pH range 4 to 12 (Meejoo et al., 2006). Previous studies have shown that HAP is an effective sorbent for

taking up heavy metals and radionuclides from solution in the environment (Meejoo et al. (2006), Corami et al. (2008), Lee et al. (2005), Xu et al. (1994), Smičiklas et al. (2006), Huang et al. (2011)). However, the sorption behavior of Sb(V) on the surface of hydroxyapatite is poorly known, including the roles of pH, Sb(V) concentration, and ionic strength. Several studies have investigated the sorption behavior of Sb(III) and Sb(V) on iron, manganese, and aluminum oxides (Rakshit et al. (2011), Xi et al. (2009), (2011), Mitsunobu et al. (2010), Wang et al. (2012a), Ilgen and Trainor (2012), Sarı et al. (2012), Li et al. (2012a), Kolbe et al. (2011b)). However, there have been no studies on the sorption behavior of Sb(V) on HAP.

In this study, the sorption behavior of Sb(V) on HAP is investigated under various physical and chemical conditions through batch sorption experiments. The objects of this study are to identify environmental conditions where Sb(V) can be effectively immobilized by HAP particles in the system and to understand the physical and chemical parameters that influence the sorption process to allow further applications to environmental settings.

PREVIOUS WORK

Hydroxyapatite is considered to be an effective sorbent for immobilizing dissolved contaminants, including metals, metalloids and radionuclides. It is available with a high specific surface area, and has relatively low solubility in the near neutral pH range in aqueous systems. Numerous studies have investigated sorption of toxic metals and radionuclides on the HAP surface, including Zn^{2+}, Cu^{2+}, Co^{2+}, Pb^{2+}, Cd^{2+}, Sr^{2+} and Ni^{2+} (Brudevold et al. (1963), Ingram et al. (1992), Lazić and Vuković (1991)).

Previous work had suggested that ion exchange between a metal cation and Ca on the HAP surface is important for their adsorption (Kukura et al., 1973), although other mechanisms have been considered, including: 1) adsorption, 2) co-precipitation, and 3) precipitation (Xu et al., 1994). The sorption behavior of anion species, such as SeO_4^{4-} and AsO_4^{3-}, are thought to involve ligand exchange or substitution for PO_4^{3-}. The presence of Ca^{2+} and PO_4^{3-} in HAP has a strong effect on the sorption behavior of cations and

anions. Furthermore, with Sb in the same group as P and As in the periodic table, it might be expected that Sb(V) behaves similarly during sorption.

The sorption behaviors of both cations and anions are dependent on pH, background electrolyte, aqueous speciation, and the surface charge of HAP. As described by Bell et al. (1972)., the surface charge of hydroxyapatite depends on pH and background electrolyte. That paper determined that the PZC of HAP with NaCl as the background electrolyte is pH 7.6 ± 0.1. Previous studies of the sorption behavior of phosphate (PO_4^{3-}) on calcite, and arsenate (AsO_4^{3-}) and selenate (SeO_4^{2-}) on HAP showed that uptake depends on the pH, with a maximum at low pH and minimal uptake at and above the PZC (Chutia et al. (2009), Monteil-Rivera et al. (1999), Duc et al. (2003)). Similar behavior can be expected for Sb(V) (Liu et al. (2010), Millero et al. (2001)).

Previous work on Fe, Al and Mn oxides confirmed that Sb(III) and Sb(V) sorption decreases with increasing pH (Wang et al. (2012b), Kolbe et al. (2011a), Rakshit et al. (2011)) and the sorption affinity of Sb(III) show the sequence MnOOH > $Al(OH)_3$ > FeOOH (Thanabalasingam and Pickering, 1990). The sorption behavior depends on ionic strength of the solution and the mineral sorbent. For example, Sb(V) sorption on gibbsite shows a significant dependence on ionic strength, yet there is just a small effect on iron-zirconium oxide (Li et al., 2012b). The sorption of Sb(V) is minimal at the PZC of of metal oxides, and both of Sb(III) and Sb(V) show the highest affinity with Mn-oxide. The oxidation state of Fe is important to sorption behavior of Sb(V) and reduced Fe has more affinity to Sb(V) compared to Sb(III).

The objects of the present study are: i) to establish the systematic sorption behavior of Sb(V) on HAP over a range of Sb concentrations, ii) to determine the sorption dependence on pH and ionic strength conditions, and iii) to constrain possible sorption mechanisms.

SAMPLES AND METHODS

Reagents and materials

The hydroxyapatite used in this study was obtained from Acros Organics. The surface area as measured by N_2 BET is 70.1 m^2g^{-1}. Powder X-ray diffraction confirmed that hydroxyapatite is the only phase present. Reagent $KSb(OH)_6$ from Alfa Aesar with 94+% purity was used to make Sb(V) stock solutions for all experiments. Because of the slow dissolution of this reagent in deionized water, stock solutions were sonicated for 24 hr before use to ensure complete dissolution. Resulting solutions were clear, and final concentrations were measured with ICP-OES. The final pH of the Sb(V) stock solution was 6.43±0.1.

Solution modeling

The program PhreeqC, which uses the database from Minteq4 (USGS) was used for modeling the initial Sb(V) solutions used for sorption experiments to predict solution speciation and saturation states with respect to potential precipitates. Calculations were performed over the range of pH and ionic strength conditions of the experiments. Table 1 shows HAP equilibrium date for dissolved species. The possible processes between Ca^{2+}, Sb(V) and background electrolyte (Na^+, Cl^-) are predicted based modeling with PhreeqC with database used for this study. At pH 9.0 and above, the solutions are predicted to be supersaturated with respect to calcite. This results from dissolution of Ca^{2+} from the HAP and CO_2 from the atmosphere into the solutions at this pH. Therefore, sorption experiments were not conducted above pH 8.0.

Pre-equilibration of Hydroxyapatite suspensions

Hydroxyapatite suspensions were prepared in two stages. HAP was aged in deionized water with NaCl as the background electrolyte for at least 7 days at ambient conditions to reach solubility equilibrium. Suspensions were aged for different ionic strength and pH conditions. Suspensions were prepared for pH 5.5, 6.0, 7.0, and 8.0. HAP particles were removed from equilibrated suspensions by filtration with 0.2µm polycarbonate membrane filter (Isopore™ Membrane Filters, LOT# R4EA59977) and combined

with fresh reagent HAP for individual sorption experiments. This procedure prevented excessive dissolution of HAP during the sorption experiments. This procedure prevented excessive dissolution of HAP during the sorption experiments. The pH of the hydroxyapatite suspensions was monitored at regular intervals and, if necessary, titrated with 0.01 M HCl and NaOH. To confirm that HAP is the sole phase in the solution after aging, XRD was used to compare solid phases before and after aging HAP. Figure 3 shows the XRD results; there is no sign of the presence of other phases except the HAP.

Sorption experiments

Batch sorption experiments were conducted with acid-cleaned 125 mL polypropylene copolymer (PPCO) bottles after confirming no uptake of Sb(V) by these bottles. Preliminary experiments at different particle loadings revealed that 1 g of HAP per liter of solution resulted in a distribution of Sb(V) between the sorbent and the solution that was well suited for analyses, and was used for all subsequent experiments.

Filtered, equilibrated solutions were prepared with 1 g/L HAP in 100 mL of solution. No change in pH was observed during preparation for solutions at pH 5.5, 6.0 and 7.0. However, a slight change was observed at pH 8.0, likely due to CO_2 exchange with the atmosphere, and was adjusted accordingly.

Initial Sb(V) concentrations over the range 50-2000 µM were used for isotherm experiments and transferred to each hydroxyapatite suspension with pipette. The pipette was calibrated to ensure accurate delivery. After introduction of Sb(V) into bottles, they were sealed and placed on a shaker table for 24 hr, with the pH of each samples measured periodically. No significant changes of pH were observed after introduction of the Sb(V) into the suspensions. All the isotherm experiments were performed in replicates under identical conditions. After 24 hr, equilibrated suspensions were filtered through 0.2 µm nylon filters and delivered to acid-cleaned 15 mL polystyrene tubes (Falcon™ Conical Centrifuge Tubes) for ICP-OES analysis.

ICP analysis

All filtered solution aliquots were measured for Sb concentration using a Thermo Sciences i-CAP 6000 series ICP-OES Calibration standards were prepared from a 1000 mg/L Antimony atomic absorption standard solution (1000mg/L Antimony, SPEC CertiPrep, Inc., PLSB7-2X). The detection limit of Sb was determined to be 1 ppm (8.2 μM) (See Appendix 1). A blank standard and 50 and 100 ppm Sb(V) solutions were selected for calibration. All standard solutions were prepared prior to each session. It was found that regular cleaning of the ICP-OES was necessary to prevent precipitation. The wavelength used for analysis was 206.83 nm. The amount of sorbed Sb(V) on HAP was calculated based on the measured amount of Sb(V) remaining in solution, by subtraction from the initial Sb(V).

X-ray diffraction analysis

Solid samples collected after filtrations were examined using powder X-ray diffraction (XRD) to identify the presence of any secondary phases. A Rigaku Ultima-IV diffractometer using Cu Kα (λ = 1.5418 Å), was used. Solid samples were prepared with 24 hr reaction time, using the same procedure as in the isotherm experiments. Samples were also collected from HAP-free solutions prepared using the same solutions from the highest concentration experiments (2000 μM) with I = 0.1 M NaCl to identify possible precipitates in the absence of HAP. Solutions were placed on a shaker table for 24 hr and then centrifuged to isolate solid particles. Solids were dried at room temperature and briefly ground with a quartz pestle and mortar for examination with XRD. A 2 theta range 10-80 degrees was used, with the glass sample plate.

RESULT

Isotherm experiment results

The results of Sb(V) sorption experiments on hydroxyapatite are presented as room-temperature isotherms in Figures 4-9. The isotherm is an effective way to show the distribution of Sb(V) between the

solution and the surface of HAP. All isotherms in this study are plotted with Sb(V) sorbed on HAP (μmol/g) as a function of remaining Sb(V) in the solution (μM). The sum of those two value corresponds to the initial [Sb(V)] (μM). The isotherms showing different ionic strengths presented in Figures 4 and 6 are shown in an enlarged view for the lower concentration range, [Sb(V)] ≤ 750 μM, in Figures 5 and 7. The isotherm trends in Figure 4 (I = 0.005 M) show that the amount of Sb(V) sorbed increases as the initial [Sb(V)] increases below 600 μM. However, above [Sb(V)] = 600 μM, the isotherms exhibit a sharp increase in uptake, which is more obviously shown at pH 7.0 and 8.0. Figure 5 shows an enlarged view of the isotherm below [Sb(V)] = 750 μM. The trend of the isotherm at I = 0.01 M (Figure 6) is mostly consistent with the isotherm from I = 0.005 M (Figure 4) at entire pH range. Particularly, above [Sb(V)] = 600 μM, both of isotherm (Figure 4 and 6) shows steep increasing at pH 7.0 and 8.0. Typical adsorption behavior was observed at pH 5.5 and 6.0, however, at pH 7.0 and 8.0, the isotherm has different adsorption behavior from both of ionic strength (Figure 5 and 7).

The isotherm results show that the behavior of Sb(V) on HAP is affected by both pH and ionic strength. Furthermore, sharply increased uptake behavior with higher Sb(V) initial concentration is suggestive of a different sorption process in the suspension. The pH dependent behavior of Sb(V) is possibly related to the point of zero charge (PZC) of HAP. These two critical factors on sorption behavior of Sb(V) will be discussed separately.

i. Influence of pH on Sb(V) sorption

The pH dependence of Sb(V) sorption was examined over the pH range 5.5-8.0 at two ionic strength conditions (0.005 and 0.01 M). Figure 4 and 6 contain the entire Sb(V) range of isotherm results and enlarged isotherms below [Sb(V)] ≤ 750 μM are in Figure 5 and 7. The pH dependence Sb(V) behavior is clearly shown in Figure 5 at relatively lower Sb(V) with I = 0.005 M. The isotherms generally show the trend that as pH increases, the amount of Sb(V) on hydroxyapatite is decreased at initial [Sb(V)] ≤ 750

μM (Figure 5). In detail, this does not hold for the pH 7.0 isotherm at I = 0.005 M above 350 μM Sb(V). These inconsistencies may result from experimental errors. However, for initial [Sb(V)] ≥ 1000 μM different behaviors are evident in Figure 4 and 6. Both of isotherm from different ionic strength (Figure 4 and 6) show a steep slope with higher initial concentration and suggests a different uptake mechanism, such as formation of a second phase. This trend shown in Figure 4 and 6 above [Sb(V)] ≥ 600 μM is evident for the entire pH range and suggests that a mechanism other than adsorption on hydroxyapatite is needed to explain behavior at high Sb(V) concentrations for both of ionic strength. Figure 6 and 7 showed the isotherm conducted with I = 0.01 M. The behavior of pH dependence is obviously observed at pH 5.5 and 6.0 because the sorbed Sb(V) decreased as pH increased. However, unlike isotherm trends at pH 5.5 and 6.0, Sb(V) behavior at pH 7.0 and 8.0 less effect at higher ionic strength (Figure 7).

ii. Influence of ionic strength on Sb(V) sorption

The behaviors of Sb(V) with different ionic strengths of NaCl are compared in Figures 8 and 9. The effect of ionic strength below 500-600 μM is minimal for all pH conditions, in as much as isotherms for both ionic strength conditions (0.005 and 0.01 M) are generally coincident at lower concentrations (Figure 8 and 9). However, ionic strength has a greater effect on Sb(V) behavior at concentrations greater than ~600-700 μM (Figure 8 and 9). In both of Figure 8 and 9, isotherms for the different ionic strengths diverge significantly at higher Sb(V) concentration for each pH condition. For pH 5.5 this ionic strength is somewhat smaller than at other pH conditions (Figure 8). The effect of ionic strength on Sb(V) uptake is different at pH 8 compared to pH 5.5, 6.0, and 7.0 (Figure 8 and 9). At these latter pH conditions, the sharp increase in uptake is enhanced at I = 0.005 M, whereas at pH 8.0 the enhancement is observed for the higher ionic strength, 0.01 M.

Both isotherms at pH 7.0 and 8.0, with I = 0.01 M, show an initial rise followed by a decrease in sorption near 500 μM. The experimental result at [Sb(V)] = 500 μM likely reflects an experimental anomaly that cannot be explained with the present data and more investigation is required.

iii. Influence of surface charge of HAP on Sb(V) sorption

Figure 10 shows the Sb(V) sorbed on HAP as a function of pH at four initial Sb(V) concentrations. For all Sb(V) concentrations, the sorbed fraction decreases with increasing pH. A distinct inflection in sorption curves (that would represent a pH edge) is not evident. Nevertheless, the decrease in sorption with increasing pH is consistent with the behavior expected for an anion. The PZC value of HAP is ~7.6 ± 0.1, and the lowest observed sorption in Figure 10 at this pH is consistent with expected behavior.

Characterization of precipitates during sorption

The isotherm results showing a sharp increase in uptake at higher Sb(V) concentrations suggest a different uptake mechanism relative to lower Sb(V) concentrations. In other studies, a sharp increase in uptake has commonly been explained as the result of surface or bulk precipitation of a second phase. As the sharp increase in uptake is dependent on ionic strength, it was considered that any precipitation process could involve a component of the background electrolyte, NaCl. Separate experiments were performed that duplicated initial solution conditions in suspensions in the absence of HAP. With no initial solid phase present, any precipitation could be identified in the filtrate following reaction. Figure 11 shows XRD results for precipitates identified in filtrates at pH 5.5 and 7. Comparison with the ICSD diffraction database reveals that the precipitate at both pH conditions is $NaSb(OH)_6$, known as the mineral mopungite.

DISCUSSION

It is well known that the sorption behaviors of both cations and anions are controlled by several factors, including pH, concentration, and background electrolyte (Hayes and Leckie, 1987). In this study, we find that all these factors exert an influence on the observed uptake behavior of Sb(V) onto HAP. The most notable finding of this study is the sharp increase in sorption at higher Sb(V) concentrations (Figures 4

and 6). This upturn, although most pronounced at pH 7.0 and 8.0, is strongly affected by ionic strength (Figures 8 and 9). We therefore consider that the presence of NaCl as the background electrolyte is one of the primary factors to control the sorption behavior of Sb(V) on HAP at higher Sb(V) concentrations. Sodium ion in solution from the NaCl electrolyte allows for precipitation between Na^+ and $Sb(OH)_6^-$ to form sodium hexa-hydroxoantimonate ($NaSb(OH)_6$), which is the mineral mopungite. To ascertain if the solution was oversaturated with respect to $NaSb(OH)_6$, we modeled initial solution conditions using PhreeqC, as described below.

Sb complexation with Na^+

The solubility of $NaSb(OH)_6$, mopungite, was reported by Blandame et al. (1974) as $K_{sp} = 8.89 * 10^{-6}$ (log K = -4.96, Table 2). Among the alkali metal hydroxoantimonates, the sodium form is the least soluble at room temperature, with the trend in solubilities $Cs^+ > Rb^+ > K^+ > Na^+ < Li^+$. This also may explain the slow dissolution of the $KSb(OH)_6$ reagent. The reported solubility product for mopungite and thermodynamic data for related species (Filella et al., 2009) were used for PhreeqC modeling of saturation states for initial solution conditions during isotherm experiments (See Table 2).

The saturation index (SI) values modeled with PhreeqC are presented in Figure 12. The SI value for mopungite is plotted as a function of initial Sb(V) in the suspension for pH 5.5 and 7.0. Values of SI > 0 represent supersaturated solution conditions and values < 0 represent undersaturated solution conditions. The SI values in Figure 12 show that mopungite precipitation is favored only for the highest Sb(V) concentration at I = 0.01 M NaCl (for both pH 5.5 and 7.0). All other initial solutions are undersaturated with respect to mopungite. However, we observe a sharp upturn in sorption at lower concentrations and lower Sb(V) concentration, which we have suggested may be due to precipitation. Hence, if the observed upturn in sorption is due to precipitation of mopungite, it occurs at a lower Sb(V) concentration and lower ionic strength than predicted by the thermodynamic calculations. There are several possible explanations for this discrepancy. First, it is known that surface precipitation may occur at lower saturation conditions

than in bulk solution. The HAP surface may facilitate such precipitation even though the calculations do not support precipitation in bulk solution. Second, we cannot rule out the possibility that the solubility product reported for mopungite is in error; there is no way to evaluate that further in this study. Finally, it is possible that surface precipitation results in a phase, possibly a mixed phase, other than mopungite. We note that XRD results described earlier indicate that mopungite does indeed precipitate at 0.1 M and 2000 μM Sb(V) at both pH 5.5 and 7. However, these conditions are not equivalent to those used in our sorption experiments. Ultimately, we are unable to resolve this discrepancy with the currently available data, and further study is required.

Sb(V) complexation with Ca^{2+}

Previous work that investigated possible precipitation reactions showed that calcium antimonates, such as $Ca[Sb(OH)_6]_2$ and $Ca_2Sb_2O_7$ (romeite), could be solubility limiting phases (Ainsworth et al. (1990), Oorts et al. (2008), Diemar et al. (2009)). The HAP-equilibrated solutions clearly contain Ca^{2+}. However, the PhreeqC calculations showed that equilibrated suspensions were undersaturated with respect to these calcium antimonate phases.

Sb(V) sorption on Hydroxyapatite

The sorption behavior of anions on mineral surfaces is controlled by multiple factors, such as pH, ionic strength, the surface charge and sites of the sorbent and background electrolyte (Stumm (1987), Sposito (1984), Parks (1990)). The results presented here show that adsorption behavior of Sb(V) on HAP depends on pH, ionic strength, Sb(V) concentration, and the background electrolyte. It is not possible to determine the maximum in adsorption (Γ_{max}) because of the occurrence of apparent precipitation at high initial Sb(V) concentration.

i) Use of nonlinear regression for Langmuir and Freundlich models

Various types of isotherms can be used to model the distribution of sorbate between the solution and the surface of the sorbent. The Langmuir and Freundlich isotherms are the most widely used types of isotherms. The Langmuir isotherm is based on the assumption of limited surface sites available for the sorbate, and this results in a plateau corresponding to the maximum adsorption. The Freundlich isotherm does not exhibit a maximum in adsorption. It is commonly used for empirical modeling of sorption behavior. The nonlinear regression function in Sigma plot 13.0 (Systat Software, Inc.) was used to model sorption data with both the Langmuir and Freundlich equations. Fit parameters for the Langmuir (K_a and B_{mzx}) and for the Freudlich (K_F and n) models were determined. Because of the sharp upturn in sorption above ~750 µM, fitting was limited to the concentration range below 750 µM . Table 3 shows the parameters obtained for both equations. Figure 13 shows both fitted isotherm models for the sorption data at pH 5.5 (I = 0.005 M) and pH 8.0 (I = 0.01 M). It is found that both models represent the sorption isotherms equally well over the limited data range shown. Furthermore, in the absence of a clear maximum in uptake, no preference in model can be identified.

Surface area and charge of hydroxyapatite

i) Surface site of hydroxyapatite

Hydroxyapatite, which was obtained from Acros (LOT#0321992, CAS : 1306-06-5), has a surface area of 70.1 m^2/g as determined by N_2 BET measurements. The desired particle loading of hydroxyapatite is 1.0 g/L. Therefore, the number of Sb(V) ions sorbed onto on HAP per unit area could be calculated. Table 4 contains calculated Sb ions per nm^2 on HAP. The number of Ca^{2+} sites on the (110) surface of HAP is 6. We estimate that this corresponds to the maximum number of potential sorption sites for Sb(V) surface complexes, and typical monolayer coverageis likely half that value. It is useful to compare the actual coverage of Sb(V) with the maximum number of available surface sites, which gives an estimation of fractional monolayer coverage. The calculated surface site coverage is less than 1 except for the higher initial Sb(V) concentrations, over the entire pH range at both ionic strength conditions (Table 4). This

result is consistent with Sb(V) adsorption at lower Sb(V) concentrations in solution and the absence of a maximum. At higher Sb(V) solution concentrations, where the calculated surface site coverage exceeds 2-3, this is consistent with surface precipitation. Therefore, the sorption of Sb(V) on the surface of HAP is likely dominated by surface precipitation at highest Sb(V) concentrations and adsorption at lower Sb(V) concentrations.

Surface charge of hydroxyapatite

The surface charge of HAP can be altered by interaction with surrounding conditions, such as background electrolyte and pH of the solution. Generally, the net surface charge of hydroxyapatite is positive at pH values below the PZC and negatively charged above the PZC (Jenne (1998), Stumm (1987)). The point of zero charge (PZC) corresponds to the pH at which the surface charge is zero. The location of the PZC can be shifted to more negative or positive directions depending on the background electrolyte concentration in the solution, and the resulting shift of PZC can influence sorption behavior of anions or cations (Sposito, 1984).

$Sb(OH)_6^-$ is the dominant aqueous species of Sb(V) in the environment, and because it has negative charge the sorption behavior of Sb(V) is affected by the location of the PZC of hydroxyapatite. Figure 10 shows that the Sb(V) sorbed on HAP depends on pH. Although there is no distinct pH edge, it is obvious that as pH increases, the sorbed Sb(V) decreases. At the PZC, little Sb(V) is sorbed on the HAP surface. At lower pH, sorption increases. This result is consistent with expected differences in surface charge as the pH changes.

CONCLUSION

The experimental results show that the sorption behavior of Sb(V) with hydroxyapatite is affected by pH and ionic strength, and strongly affected by type and concentration of background electrolyte. Similar with the behavior exhibited by other anions, Sb(V) adsorption decreases as pH increases, which reflects

the influence of decreasing positive surface charge. The presence of NaCl background electrolyte exerts an effect on sorption at higher Sb(V) concentration. In this study, this is caused by the formation of a secondary phase. Precipitation of NaSb(OH)6, mopungite, considerably affects the behavior of Sb(V) at higher [Sb(V)]. .

Equally good fits of Langmuir and Freundlich isotherm models are obtained for the sorption data below 750 µM. The calculated Sb surface coverage on HAP suggest that surface precipitation of Sb(V) on HAP is dominant at higher Sb(V) concentration. Therefore, it is possible to speculate that in the presence of NaCl solutions the sorption mechanism of Sb(V) on HAP is dominantly by precipitation at higher Sb(V) concentration. At lower Sb(V) concentrations, or in the absence of dissolved NaCl, the immobilization of Sb(V) may occur by formation of surface complexes on the HAP surface. However, spectroscopic study would be needed to confirm such a mechanism The desorption behavior of Sb(V) on HAP surface also remains unexplored. Therefore, the stabilization of Sb(V) by HAP should be investigated for before using HAP as a sorbent.

Even though much research has focused on the sorption behavior of Sb species in solution with various minerals under a range of conditions, the fate and movement of Sb(V) in nature is still largely unknown (Filella et al., 2002c). Like As, there is no known biological function for Sb in the human body, and it is considered toxic. Lack of understanding of Sb could result in environmental issues, such as human health problems and contamination in soil and water. The occurrence of Sb in natural waters is poorly understood. Based on the experimental results in this study, a reaction with alkali elements is potentially important and could result in formation of an insoluble compound. This could be a critical factor for constraining the behavior of Sb(V) in environmental settings. In environmental settings there are various factors that affect the behavior of Sb(V) and related species. More biologically related research should be focused on understanding the behavior of Sb, such as oxidation reactions between Sb(III) and Sb(V), as

well as methylation related to biological process and the solubility of Sb in natural water to constrain the transport of Sb in nature.

References

Ainsworth, N., Cooke, J. and Johnson, M. (1990) Distribution of antimony in contaminated grassland: 1—vegetation and soils. Environmental pollution 65, 65-77.

Bell, L.C., Posner, A.M. and Quirk, J.P. (1972) Surface Charge Characteristics of Hydroxyapatite and Fluorapatite. Nature 239, 515-517.

Blandame.Mj, Burgess, J. and Peacock, R.D. (1974) Solubility of Sodium Hexahydroxoantimonate in Water and in Mixed Aqueous Solvents. J Chem Soc Dalton, 1084-1086.

Brudevold, F., Steadman, L.T., Spinelli, M.A., Amdur, B.H. and Gron, P. (1963) A study of zinc in human teeth. Archives of oral biology 8, 135-144.

Chutia, P., Kato, S., Kojima, T. and Satokawa, S. (2009) Arsenic adsorption from aqueous solution on synthetic zeolites. J Hazard Mater 162, 440-447.

Corami, A., Mignardi, S. and Ferrini, V. (2008) Cadmium removal from single- and multi-metal (Cd + Pb + Zn + Cu) solutions by sorption on hydroxyapatite. Journal of colloid and interface science 317, 402-408.

Diemar, G.A., Filella, M., Leverett, P. and Williams, P.A. (2009) Dispersion of antimony from oxidizing ore deposits. Pure and Applied Chemistry 81.

Duc, M., Lefevre, G., Fedoroff, M., Jeanjean, J., Rouchaud, J.C., Monteil-Rivera, F., Dumonceau, J. and Milonjic, S. (2003) Sorption of selenium anionic species on apatites and iron oxides from aqueous solutions. J Environ Radioactiv 70, 61-72.

Filella, M., Belzile, N. and Chen, Y.-W. (2002a) Antimony in the environment: a review focused on natural waters II. Relevant solution chemistry. Earth-Science Reviews, 265.

Filella, M., Belzile, N. and Chen, Y.-W. (2002b) Antimony in the environment: a review focused on natural waters: I. Occurrence. Earth-Science Reviews 57, 125-176.

Filella, M., Belzile, N. and Chen, Y.W. (2002c) Antimony in the environment: a review focused on natural waters I. Occurrence. Earth-Science Reviews 57, 125-176.

Filella, M., Williams, P.A. and Belzile, N. (2009) Antimony in the environment: knowns and unknowns. Environ Chem 6, 95-105.

Hayes, K. and Leckie, J. (1987) Modeling ionic strength effects on cation adsorption at hydrous oxide/solution interfaces. Journal of colloid and interface science 115, 564-572.

Hem, J.D. (1977) Reactions of metal ions at surfaces of hydrous iron oxide. Geochimica et Cosmochimica Acta 41, 527-538.

Huang, Y., Chen, L. and Wang, H. (2011) Removal of Co(II) from aqueous solution by using hydroxyapatite. Journal of Radioanalytical and Nuclear Chemistry 291, 777-785.

Ilgen, A.G. and Trainor, T.P. (2012) Sb(III) and Sb(V) sorption onto Al-rich phases: hydrous Al oxide and the clay minerals kaolinite KGa-1b and oxidized and reduced nontronite NAu-1. Environmental science & technology 46, 843-851.

Ingram, G.S., Horay, C.P. and Stead, W.J. (1992) Interaction of zinc with dental mineral. Caries research 26, 248-253.

Jenne, E.A. (1998) Adsorption of metals by geomedia: data analysis, modeling, controlling factors, and related issues. Academic Press: San Diego.

Kolbe, F., Weiss, H., Morgenstern, P., Wennrich, R., Lorenz, W., Schurk, K., Stanjek, H. and Daus, B. (2011a) Sorption of aqueous antimony and arsenic species onto akaganeite. J Colloid Interf Sci 357, 460-465.

Kolbe, F., Weiss, H., Morgenstern, P., Wennrich, R., Lorenz, W., Schurk, K., Stanjek, H. and Daus, B. (2011b) Sorption of aqueous antimony and arsenic species onto akaganeite. Journal of colloid and interface science 357, 460-465.

Kukura, M., Bell, L., Posner, A.M. and Quirk, J. (1973) Kinetics of isotope exchange on hydroxyapatite. Soil Science Society of America Journal 37, 364-366.

Lazić, S. and Vuković, Ž. (1991) Ion exchange of strontium on synthetic hydroxyapatite. Journal of Radioanalytical and Nuclear Chemistry 149, 161-168.

Lee, Y.J., Elzinga, E.J. and Reeder, R.J. (2005) Sorption mechanisms of zinc on hydroxyapatite: systematic uptake studies and EXAFS spectroscopy analysis. Environmental science & technology 39, 4042-4048.

Li, X., Dou, X. and Li, J. (2012a) Antimony(V) removal from water by iron-zirconium bimetal oxide: Performance and mechanism. Journal of Environmental Sciences 24, 1197-1203.

Li, X.H., Dou, X.M. and Li, J.Q. (2012b) Antimony(V) removal from water by iron-zirconium bimetal oxide: Performance and mechanism. J Environ Sci-China 24, 1197-1203.

Liu, G., Talley, J.W., Na, C.Z., Larson, S.L. and Wolfe, L.G. (2010) Copper Doping Improves Hydroxyapatite Sorption for Arsenate in Simulated Groundwaters. Environ Sci Technol 44, 1366-1372.

Meejoo, S., Maneeprakorn, W. and Winotai, P. (2006) Phase and thermal stability of nanocrystalline hydroxyapatite prepared via microwave heating. Thermochimica Acta 447, 115-120.

Millero, F., Huang, F., Zhu, X.R., Liu, X.W. and Zhang, J.Z. (2001) Adsorption and desorption of phosphate on calcite and aragonite in seawater. Aquat Geochem 7, 33-56.

Mitsunobu, S., Takahashi, Y., Terada, Y. and Sakata, M. (2010) Antimony(V) Incorporation into Synthetic Ferrihydrite, Goethite, and Natural Iron Oxyhydroxides. Environmental science & technology 44, 3712-3718.

Monteil-Rivera, F., Masset, S., Dumonceau, J., Fedoroff, M. and Jeanjean, J. (1999) Sorption of selenite ions on hydroxyapatite. J Mater Sci Lett 18, 1143-1145.

Oorts, K., Smolders, E., Degryse, F., Buekers, J., Gasco, G., Cornelis, G. and Mertens, J. (2008) Solubility and toxicity of antimony trioxide (Sb2O3) in soil. Environmental science & technology 42, 4378-4383.

Parks, G. (1990) Surface energy and adsorption at mineral/water interfaces; an introduction. Reviews in Mineralogy and Geochemistry 23, 133-175.

Rakshit, S., Sarkar, D., Punamiya, P. and Datta, R. (2011) Antimony sorption at gibbsite-water interface. Chemosphere 84, 480-483.

Sarı, A., Şahinoğlu, G. and Tüzen, M. (2012) Antimony(III) Adsorption from Aqueous Solution Using Raw Perlite and Mn-Modified Perlite: Equilibrium, Thermodynamic, and Kinetic Studies. Industrial & Engineering Chemistry Research 51, 6877-6886.

Smičiklas, I., Dimović, S., Plećaš, I. and Mitrić, M. (2006) Removal of Co< sup> 2+</sup> from aqueous solutions by hydroxyapatite. Water research 40, 2267-2274.

Smith, K.S. (1999) Metal sorption on mineral surfaces: an overview with examples relating to mineral deposits. The Environmental Geochemistry of Mineral Deposits. Part B: Case Studies and Research Topics 6, 161-182.

Sposito, G. (1984) The surface chemistry of soils. Oxford University Press.

Stumm, W. (1987) Aquatic Surface Chemistry: Chemical Processes at the Particle-Water Interface. Wiley.

Thanabalasingam, P. and Pickering, W.F. (1990) Specific Sorption of Antimony(Iii) by the Hydrous Oxides of Mn, Fe, and Ai. Water Air Soil Poll 49, 175-185.

Wang, X., He, M., Lin, C., Gao, Y. and Zheng, L. (2012a) Antimony(III) oxidation and antimony(V) adsorption reactions on synthetic manganite. Chemie der Erde - Geochemistry 72, 41-47.

Wang, X.Q., He, M.C., Lin, C.Y., Gao, Y.X. and Zheng, L. (2012b) Antimony(III) oxidation and antimony(V) adsorption reactions on synthetic manganite. Chem Erde-Geochem 72, 41-47.

Xi, J., He, M. and Lin, C. (2009) Adsorption of antimony(V) on kaolinite as a function of pH, ionic strength and humic acid. Environmental Earth Sciences 60, 715-722.

Xi, J., He, M. and Lin, C. (2011) Adsorption of antimony(III) and antimony(V) on bentonite: Kinetics, thermodynamics and anion competition. Microchemical Journal 97, 85-91.

Xu, Y., Schwartz, F.W. and Traina, S.J. (1994) Sorption of zn2+ and cd2+ on hydroxyapatite surfaces. Environmental science & technology 28, 1472-1480.

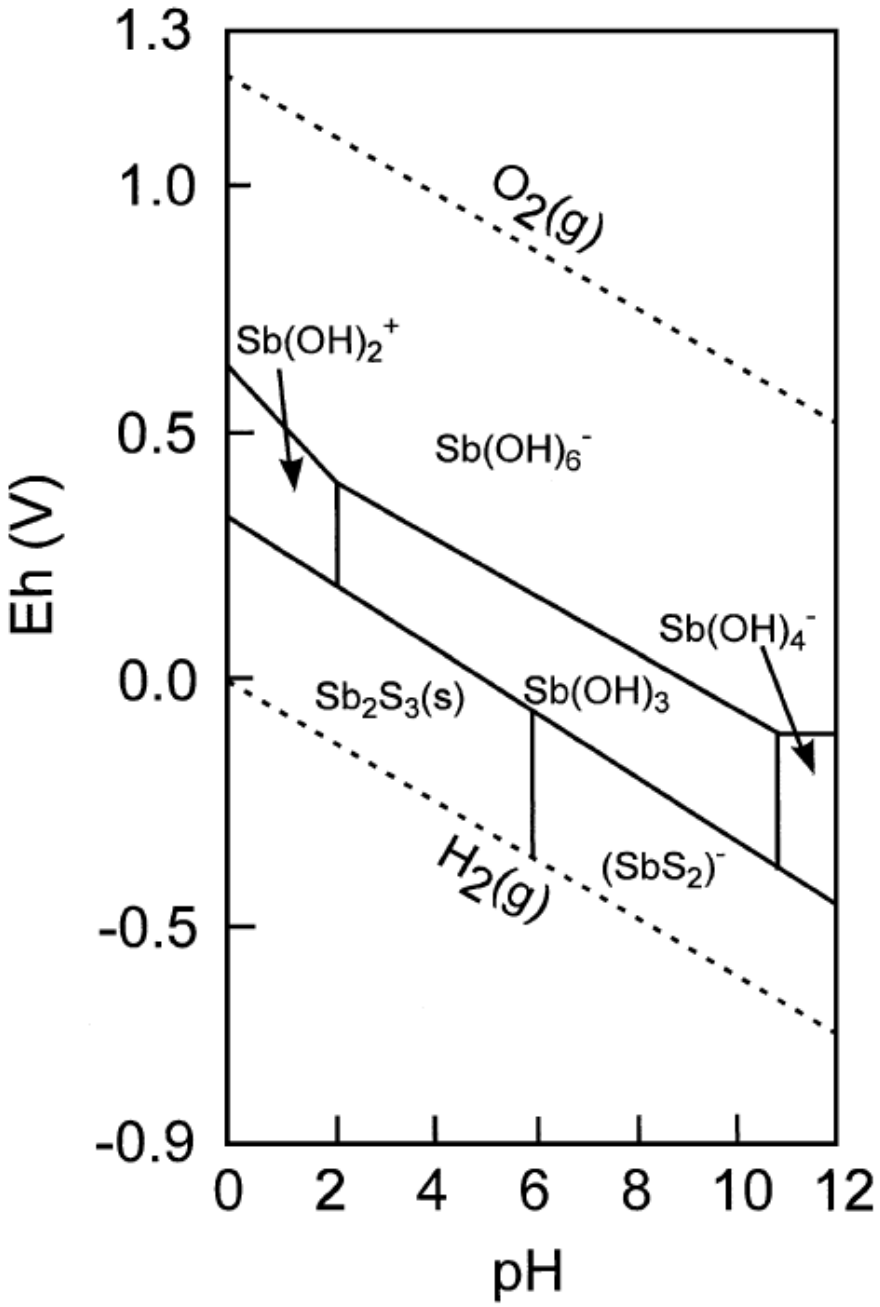

Figure 1. Eh-pH diagram of Sb ($[\sum Sb] = 10^{-8}$ mol/l $[\sum S] = 10^{-3}$ mol/) (Filella et al., 2002a)

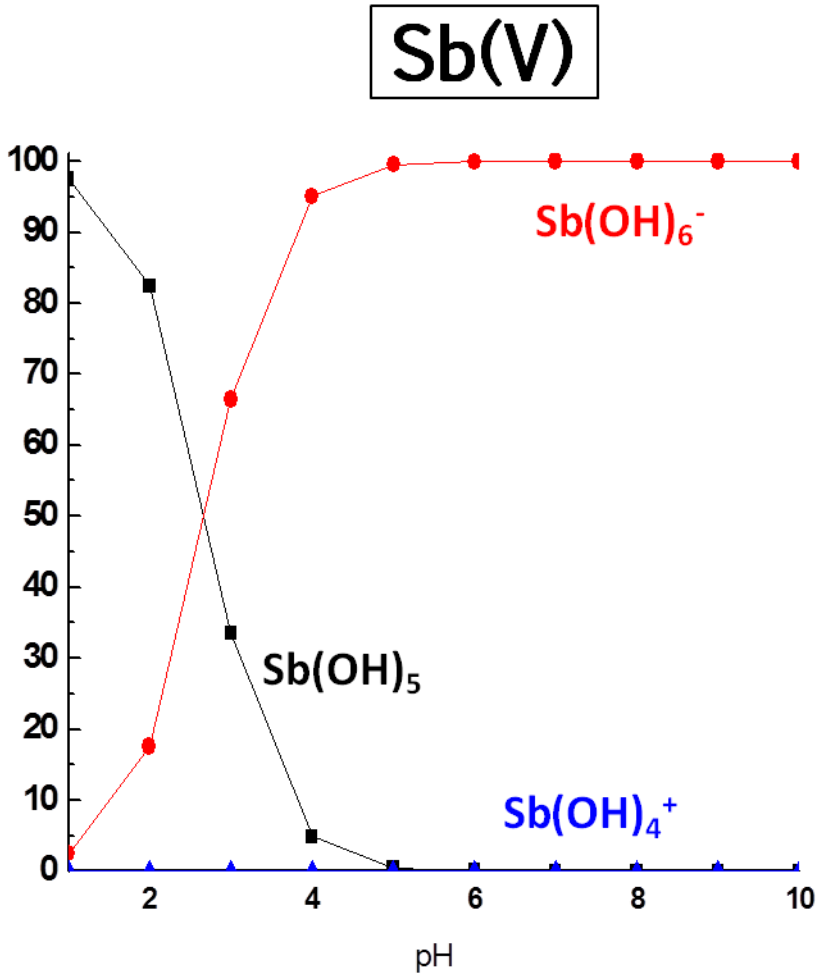

Figure 2. Sb(V) aqueous speciation from pH 1.0 to 10.0 ([∑Sb(V) = 10^{-6}], calculated with PhreeqC)

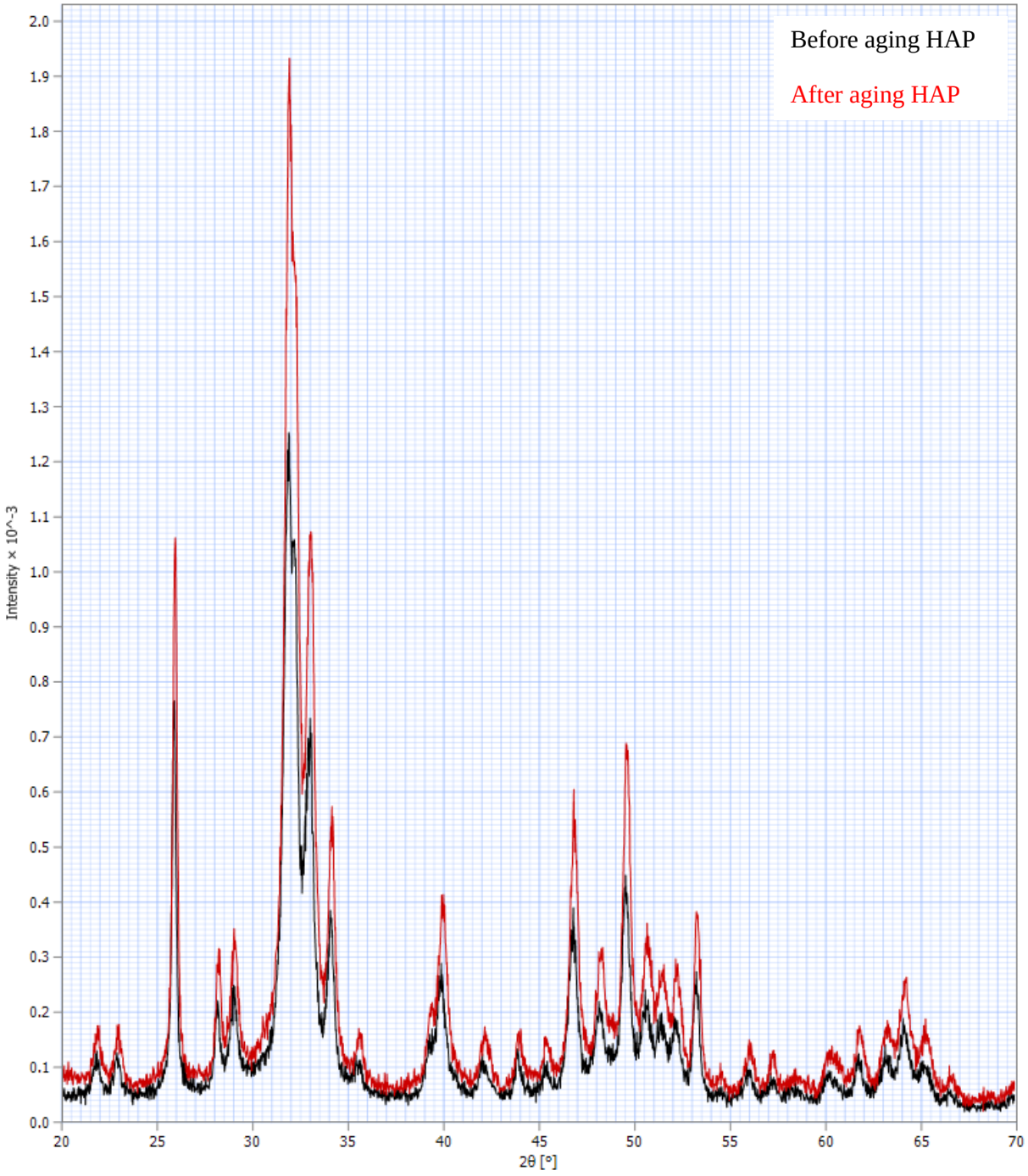

Figure 3. HAP XRD comparison before aging and after aging reagent

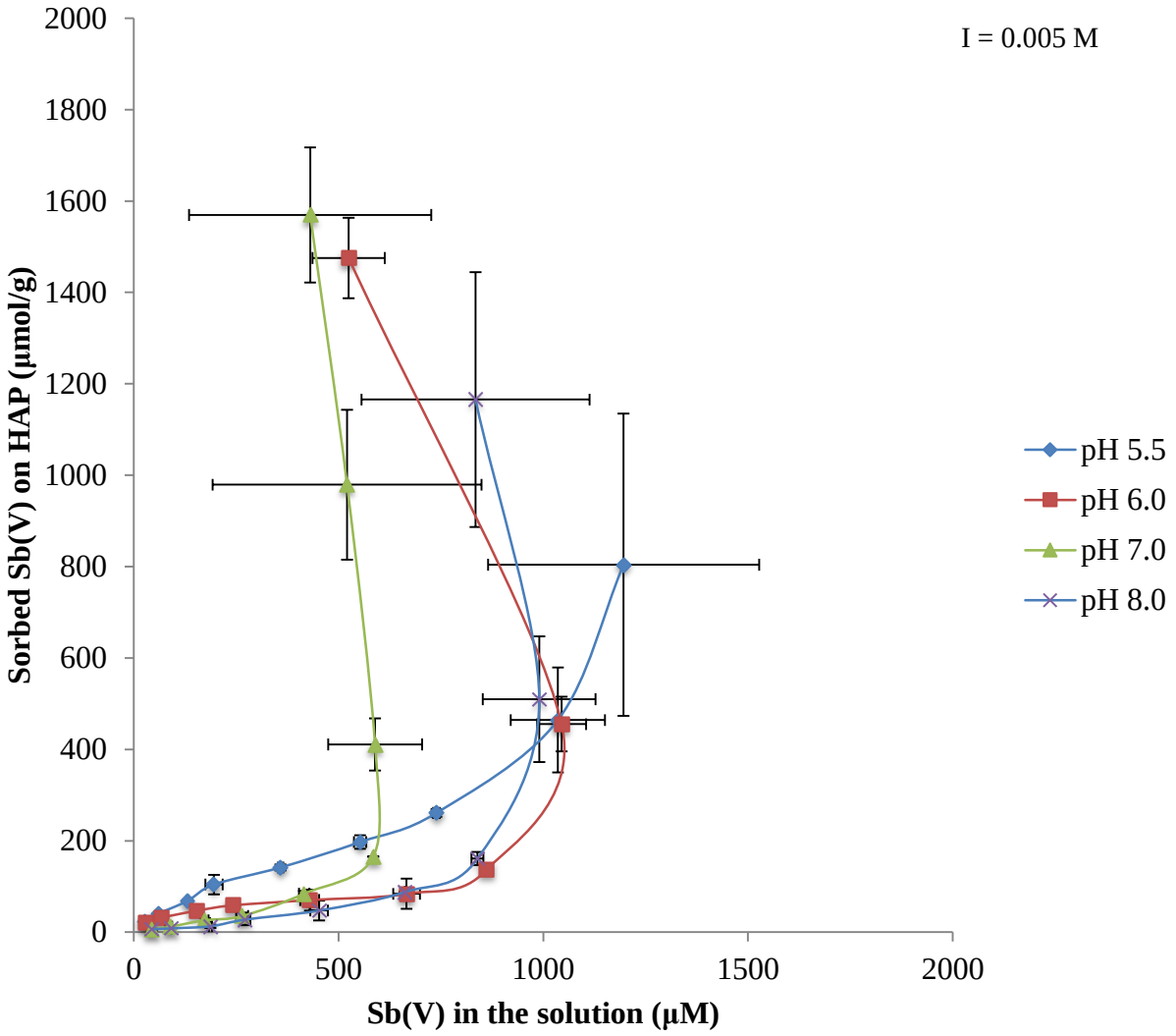

Figure 4. Sb(V) isotherm from pH 5.5 to 8.0 (I = 0.005 M)

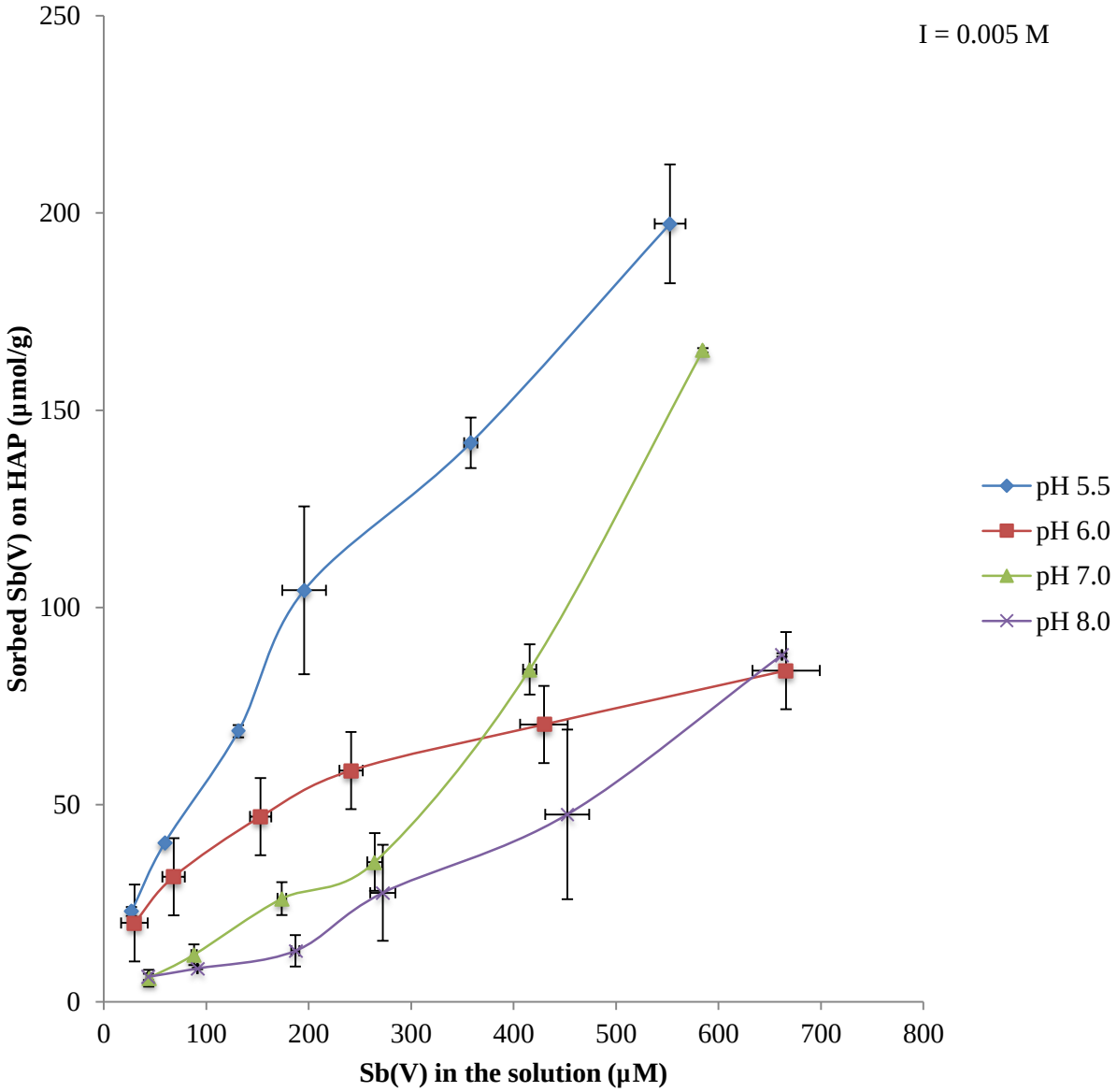

Figure 5. Enlarged Sb(V) isotherm below [Sb(V)] ≤ 750µM for all pH values

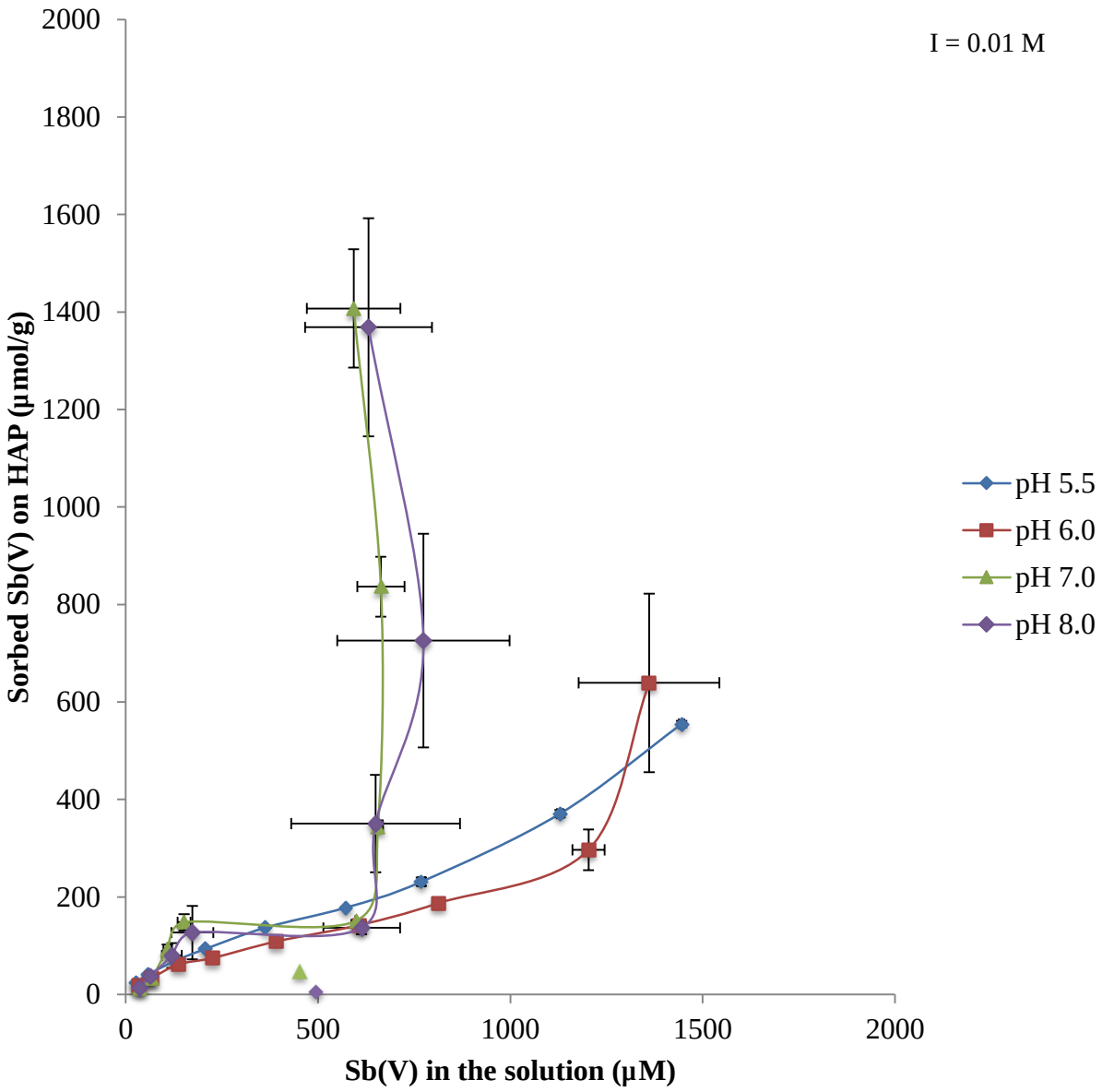

Figure 6. Sb(V) isotherms from pH 5.5 to 8.0 (I = 0.01 M)

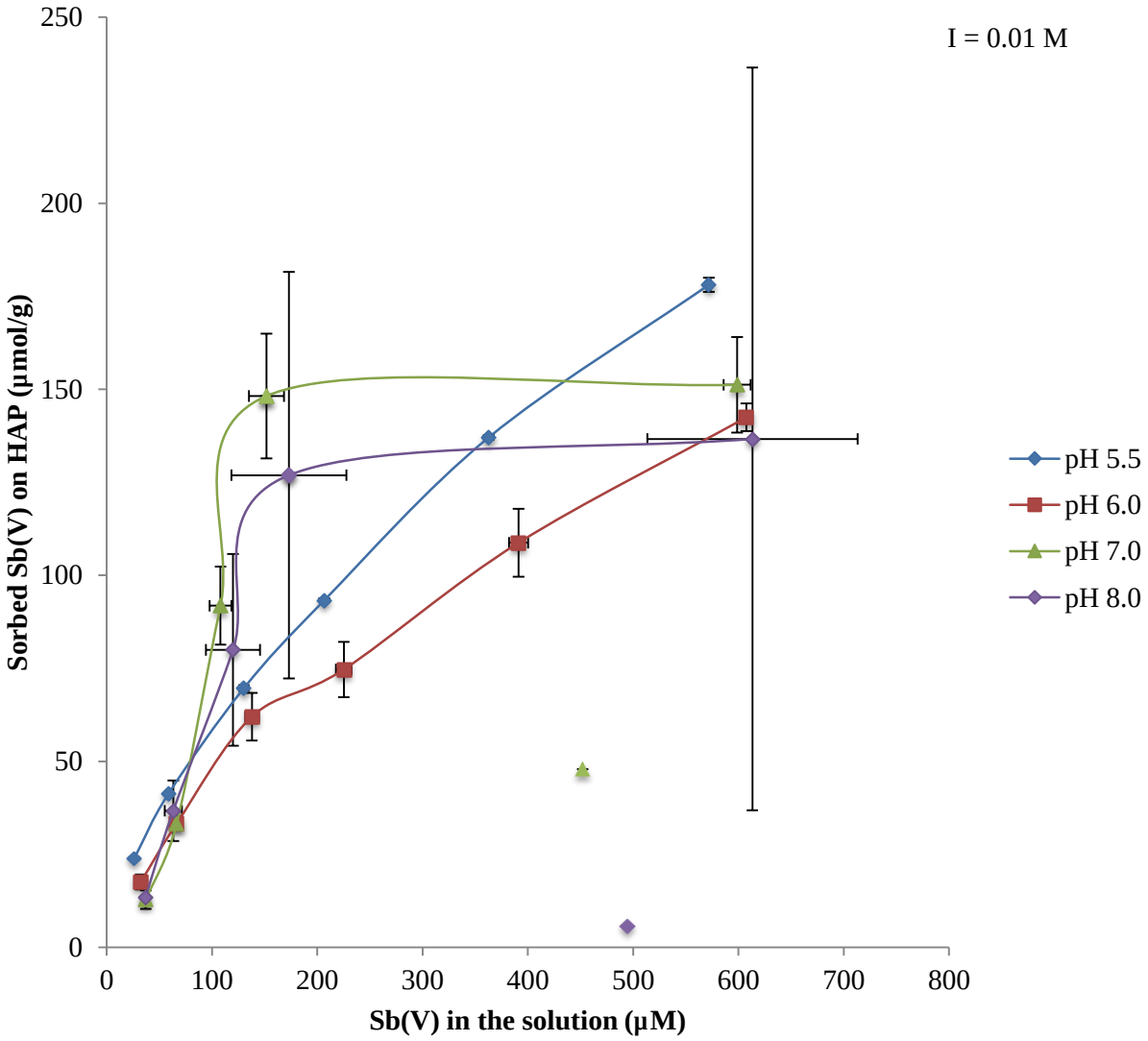

Figure 7. Enlarged Sb(V) isotherms below [Sb(V)] ≤ 750µM for all pH values

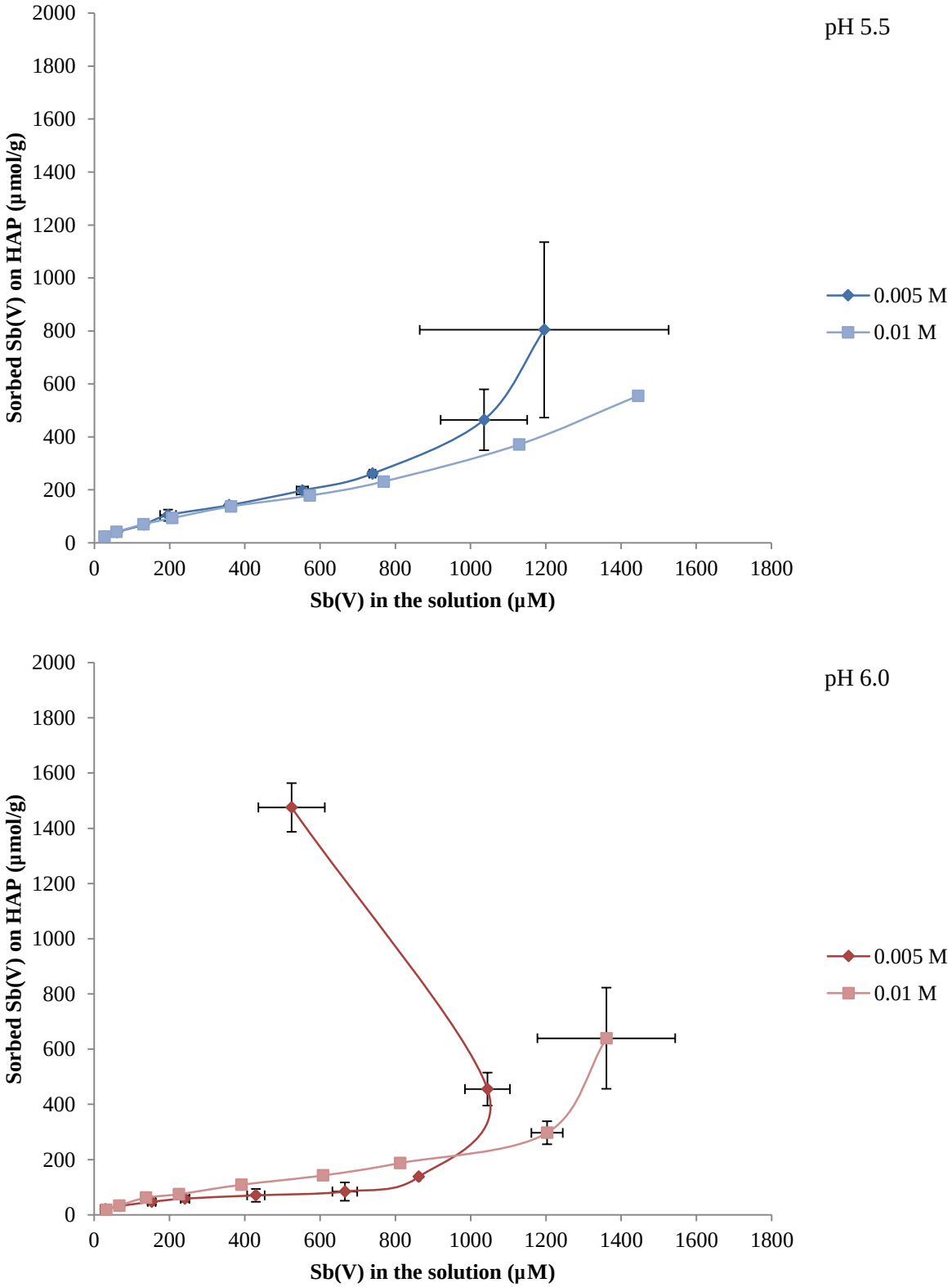

Figure 8. Isotherm comparison with different ionic strength at same pH

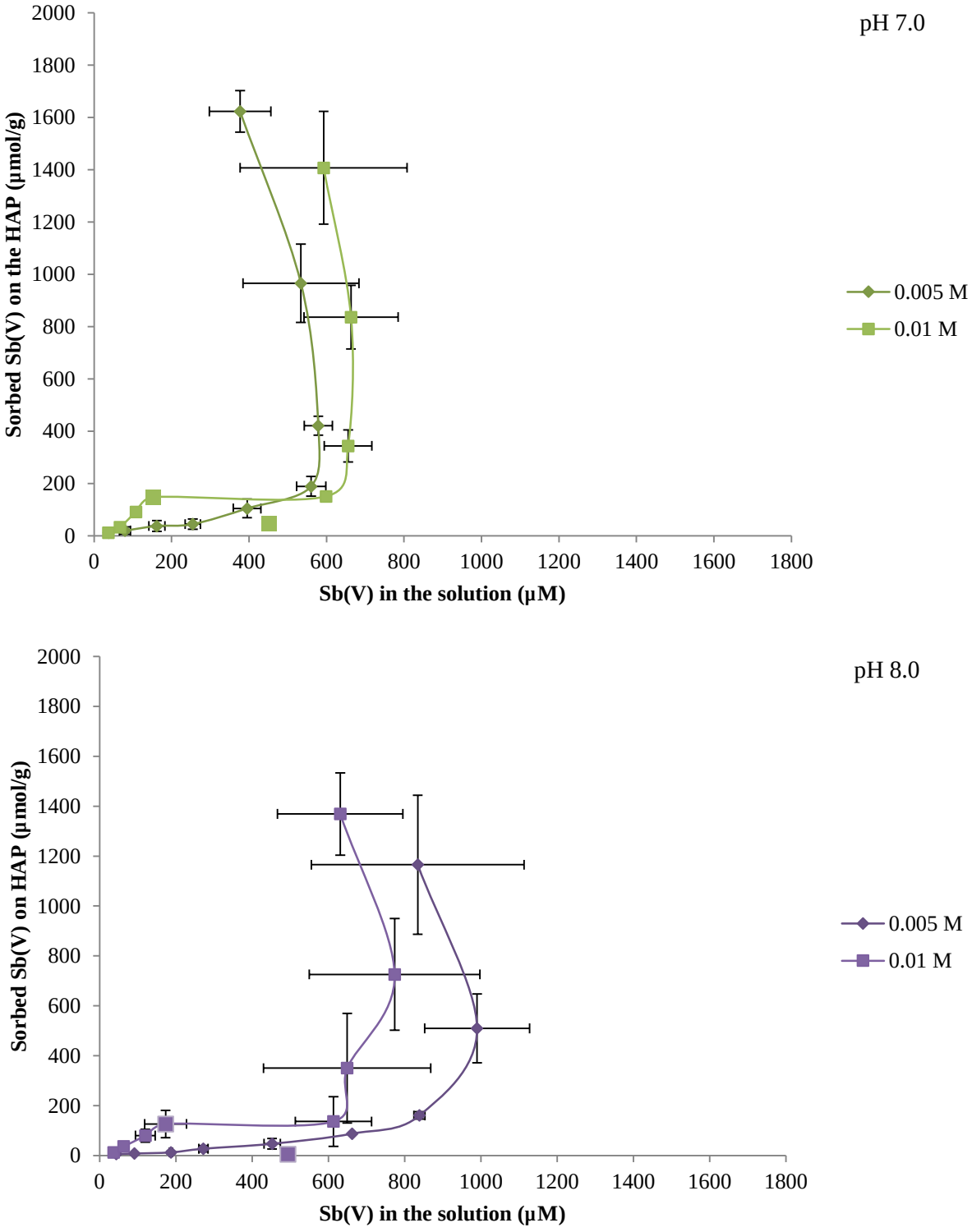

Figure 9. Isotherm comparison with different ionic strength at same pH

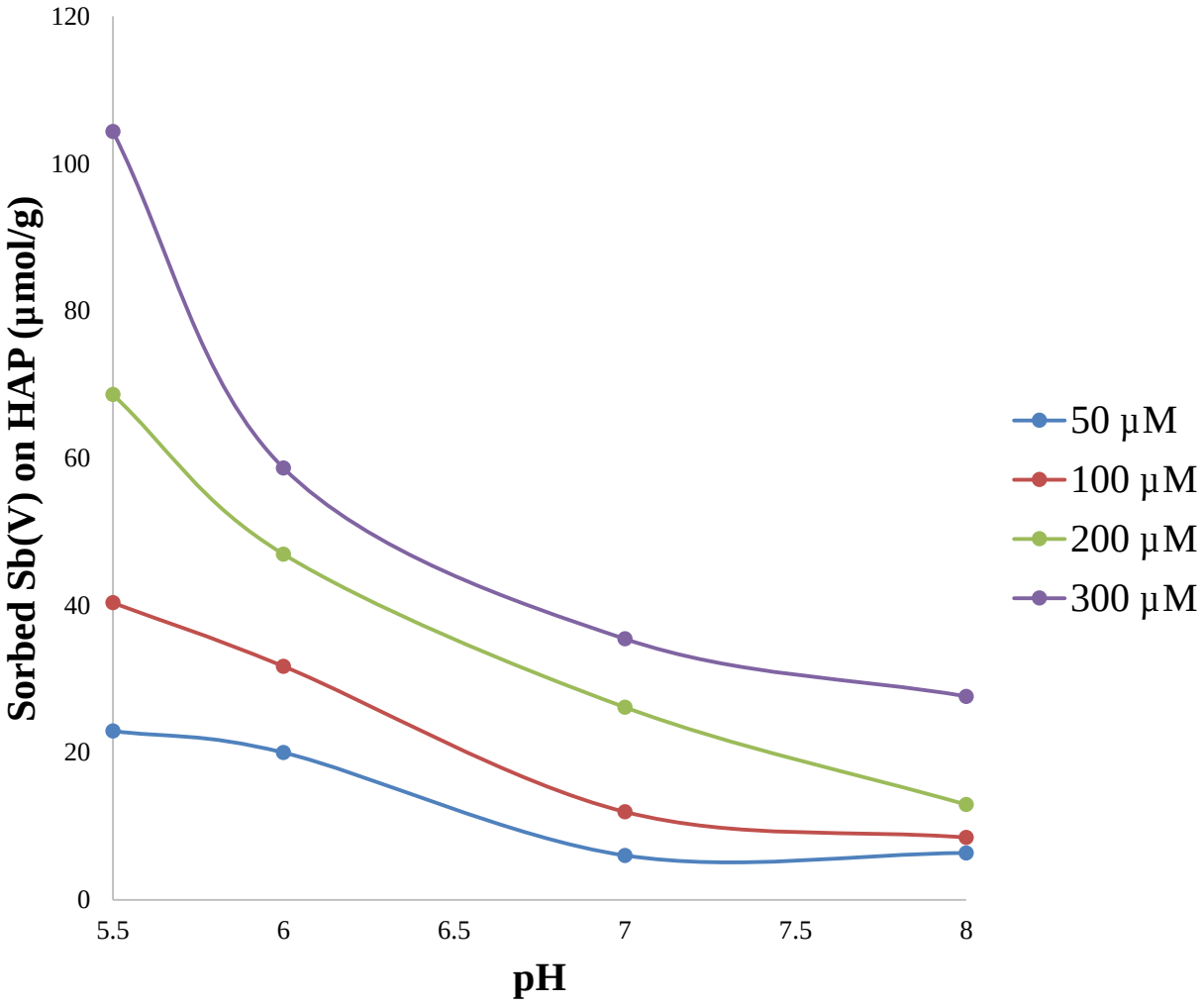

Figure 10. Sorbed Sb(V) on HAP as a function of pH (I = 0.005 M)

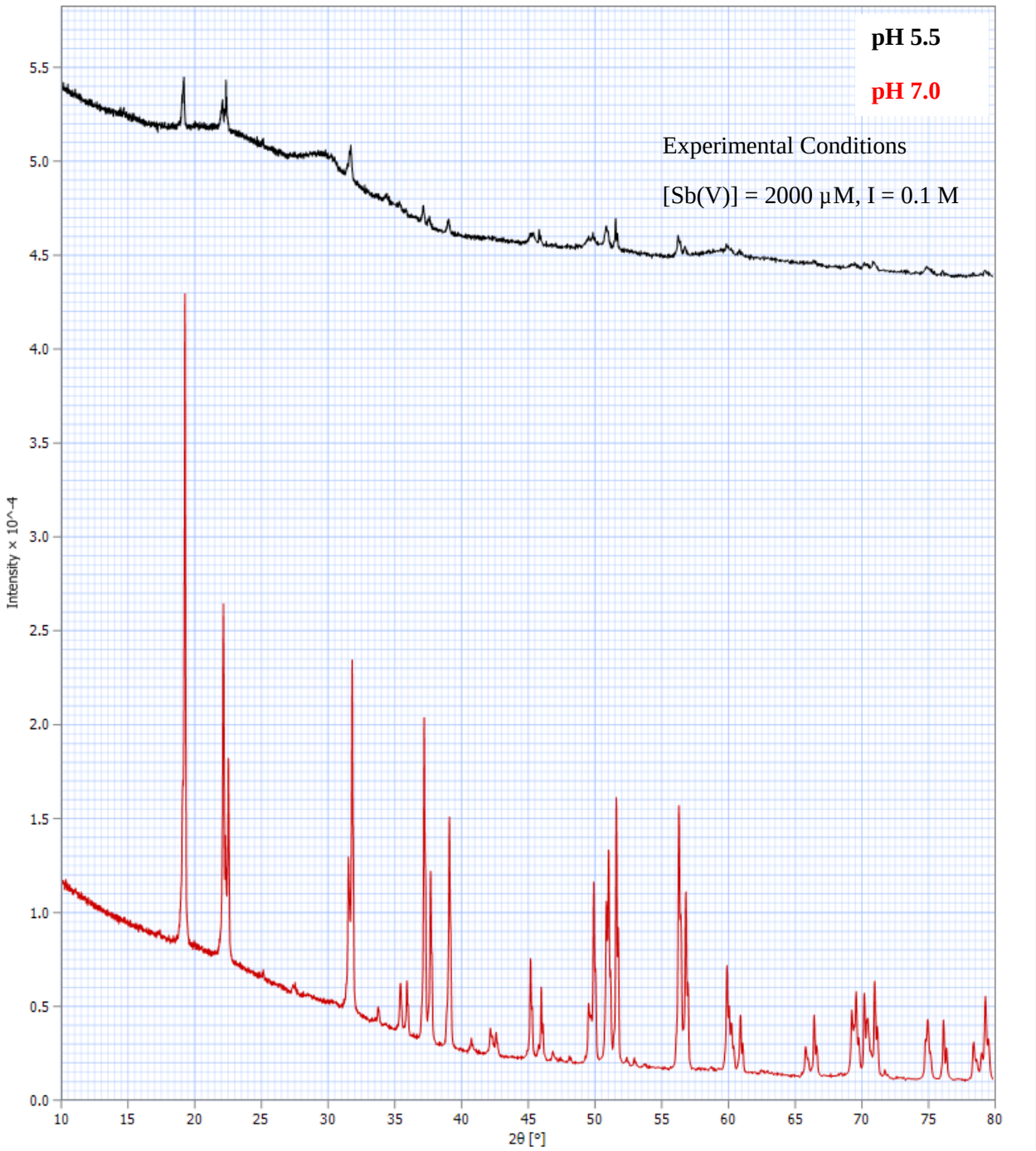

Figure 11. XRD Experimental result of solid precipitation at pH 5.5 and 7.0 ([Sb(V)] = 2000 µM, I = 0.1 M). The peaks correspond to $NaSb(OH)_6$.

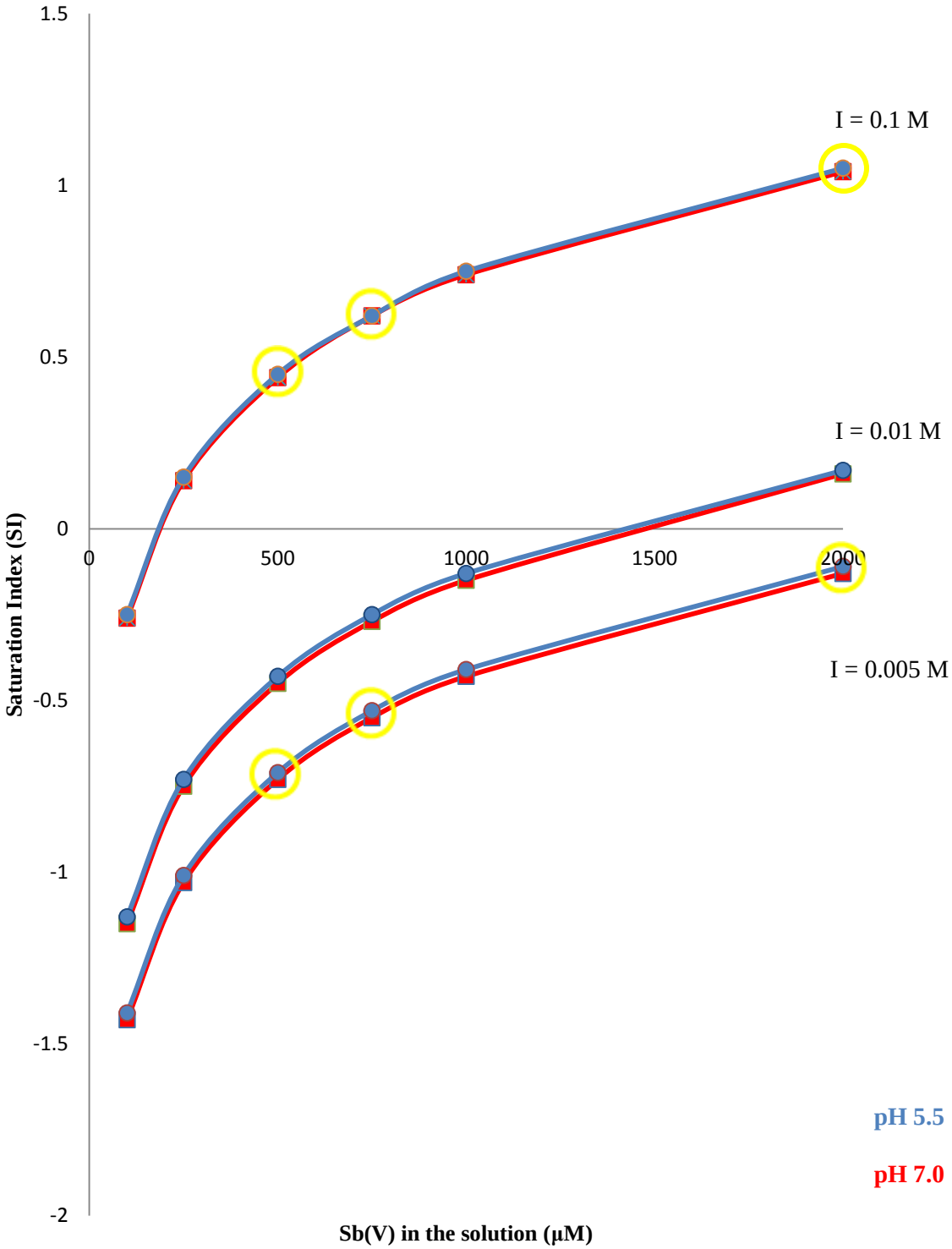

Figure 12. Saturation Index (SI) of value for $NaSb(OH)_6$ modeled with PhreeqC (experimental results are marked)

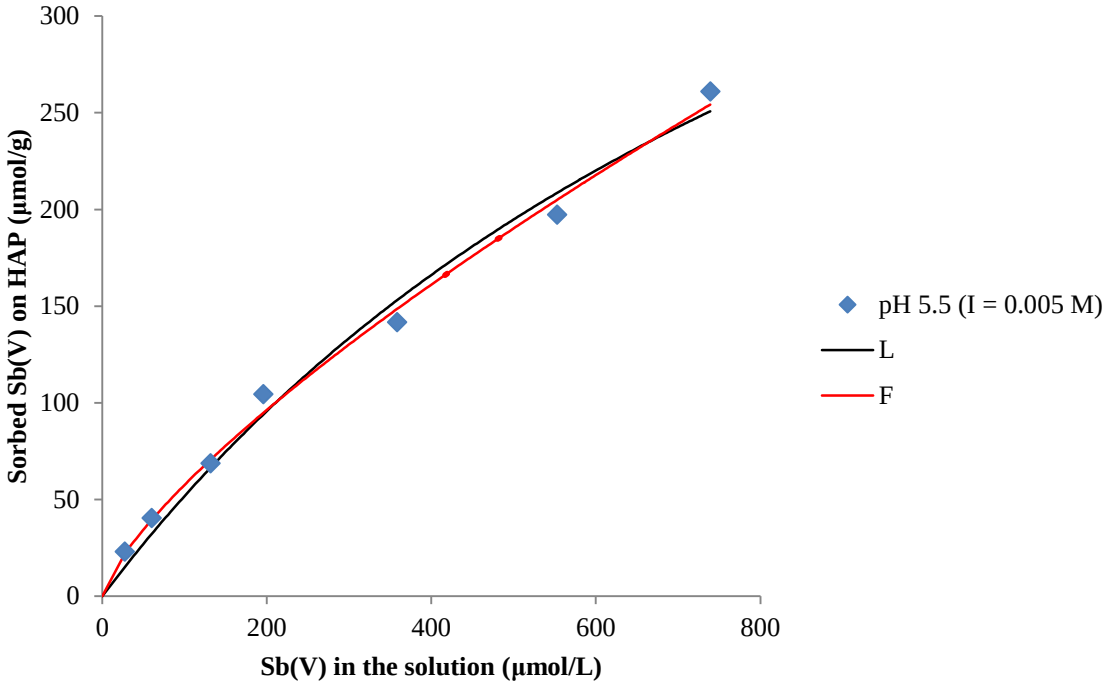

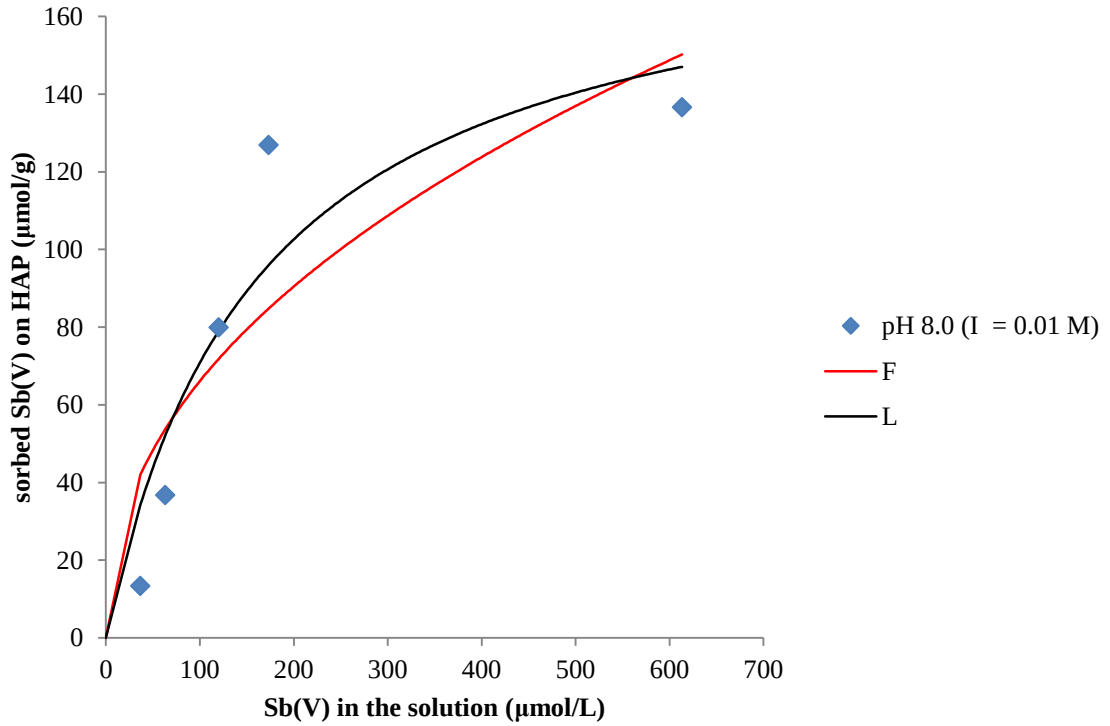

Figure 13. Use of non linear regression for the Langmuir and Freudlich models (pH 5.5, I = 0.005 M, pH 8.0, I = 0.01 M)

Table 1. HAP Equilibrium Data

Reactions	log K
$H^+ + H_2PO_4 \leftrightarrow H_3PO_4$	2.21
$H^+ + HPO_4^{2-} \leftrightarrow H_2PO_4^-$	7.81
$H^+ + PO_4^{3-} \leftrightarrow HPO_4^{2-}$	12.18
$Ca^{2+} + H2PO_4^{2-} \leftrightarrow CaH_2PO_4^+$	1.5
$Ca^{2+} + HPO_4^{2-} \leftrightarrow CaHPO_4$	2.83
$Ca^{2+} + PO_4^{3-} \leftrightarrow CaPO_4$-	6.54
$Ca_5(PO_4)_3OH \leftrightarrow 5Ca^{2+} + 3PO_4^{3-} + OH^-$	59

Table 2. Sb(V) related Solid Phase

Solid	Reaction	log K	
Pyroantimonates	$Ca_2Sb_2O_7 + 2H^+ + 5H_2O = 2Ca^{2+} + 2Sb(OH)_6^-$	- 6.7	(G. Cornelis et al. 2011)
Romeite	$Ca(Sb(OH)_6)_2 = Ca^{2+} + 2Sb(OH)_6^-$	-12.55	(G. Cornelis et al. 2011)
Mopungite	$NaSb(OH)_6 = Na^+ + Sb(OH)_6^-$	- 4.95	(Blandame.Mj et al., 1974)

Table 3. Calculated parameters form Langmuir and Freundlich isotherm

		Langmuir isotherm parameters				
pH	I = 0.005 M	B_{max}	K_d	I = 0.01 M	B_{max}	K_d
5.5		401.93	598.44		440.43	759.80
6		99.00	158.04		358.57	824.13
7		92.73	259.05		206.43	152.28
8		N.D.	N.D.		186.01	162.57

		Freundlich isotherm parameters				
pH	I = 0.005 M	K_F	n	I = 0.01 M	K_F	n
5.5		1.88	0.74		2.57	0.67
6		5.38	0.43		0.90	0.41
7		1.12	0.67		9.80	0.44
8		8.23	0.45		8.23	0.45

Table 4. **Calculated Sb/nm^2 on HAP**

	Site Density			
I = 0.005 M	pH5.5	pH 6.0	pH 7.0	pH 8.0
μM	Sb/nm^2			
50	0.20	0.17	0.05	0.05
100	0.35	0.27	0.10	0.07
200	0.59	0.40	0.23	0.11
300	0.90	0.50	0.30	0.24
500	1.22	0.61	0.72	0.41
750	1.70	0.72	1.42	0.76
1000	2.25	1.18	3.54	1.39
1500	4.00	3.92	8.43	4.39
2000	6.92	12.69	13.50	10.03

	Site Density			
I = 0.01 M	pH5.5	pH 6.0	pH 7.0	pH 8.0
μM	Sb/nm^2			
50	0.21	0.15	0.11	0.11
100	0.36	0.29	0.29	0.32
200	0.60	0.53	0.79	0.69
300	0.80	0.64	1.28	1.09
500	1.18	0.94	0.41	0.05
750	1.53	1.23	1.30	1.18
1000	1.99	1.61	2.96	3.02
1500	3.19	2.55	7.28	6.25
2000	4.77	5.50	12.11	11.78

Appendix 1.

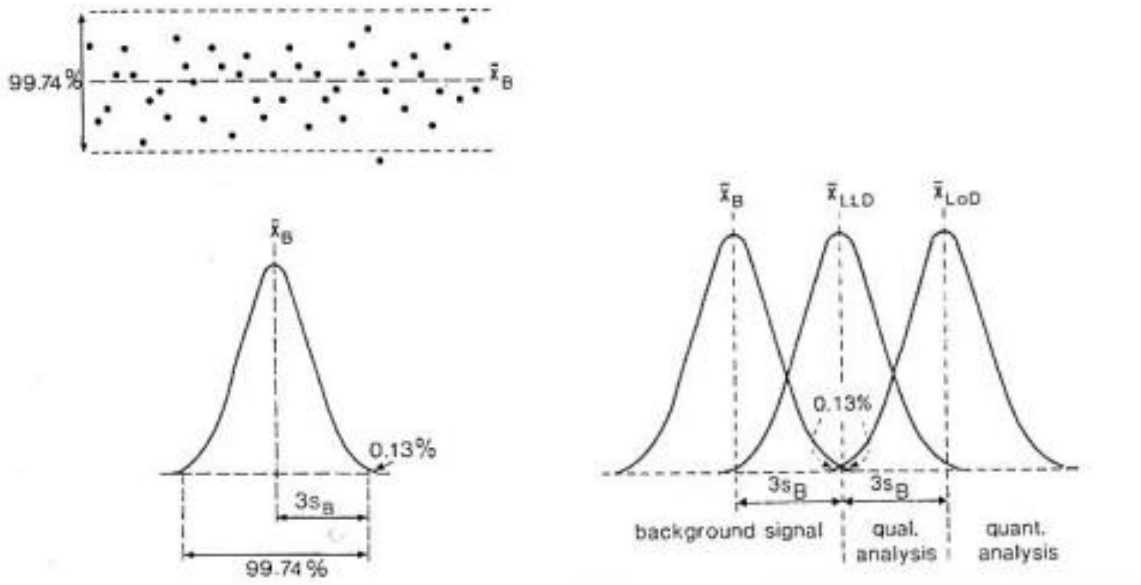

Figure 1. L: The distribution of measured value of background signals and the standard deviation with Gaussian shape. R: The relation between x_B, x_{LLD} and x_{LoD}.

Introduction

Detection limit can be broadly defined as the minimum concentration of an element that can be measured with an analytical technique. This concept can be further parsed out into a lower limit of detection (LLD) and a limit of determination (LoD), where the former term refers to the lowest concentration at which an unambiguous detection of measurable signal can be made, and the latter refers to the lowest concentration at which the concentration can be reliably quantified (Potts, 1987, *A Handbook of Silicate Rock Analysis*).

Diagrams reproduced from Potts, 1987 (Figure 1, below) illustrate the general concepts for the determination of LoD and LLD: (1) the detection limit signal should be placed on a randomly measured background measurement. (2) The measurements should show a normal distribution characterized by a mean background signal μ_B and a standard deviation δ_B. (3) The detection limit can be determined with x_B and δ_B. Figure 1 presents the relation among lower limit of detection (x_{LLD}), limit of determination (x_{LOD}), and the background (x_B).

At the lower limit of detection (x_{LLD}), the concentration of the element cannot be reliably determined, but a signal can be measured. This signal has a value of xB + 3δB. The limit of determination (x_{LoD}), which can be used for quantification, is the measurement that shows the value of xB + 6δB above the background.

In this study, we determined the LoD (as defined by Potts, 1987) for antimony on the iCAP 6000 ICP-OES using the set of measurements described below. Our results for this series of measurements are in shown on Figure 2.

Method

i) Measured a solution with Sb(V) in a known concentration (50 ppm) 3 times.
ii) Measured a blank solution 20 times
iii) Calculated the average value of 20 blank measurements and +/- standard deviation from the measurement.
iv) Calculate the limit of detection with the equation.
v) Calculated the limit of detection for Sb(V) is 0.90ppm (= 7.31µM)

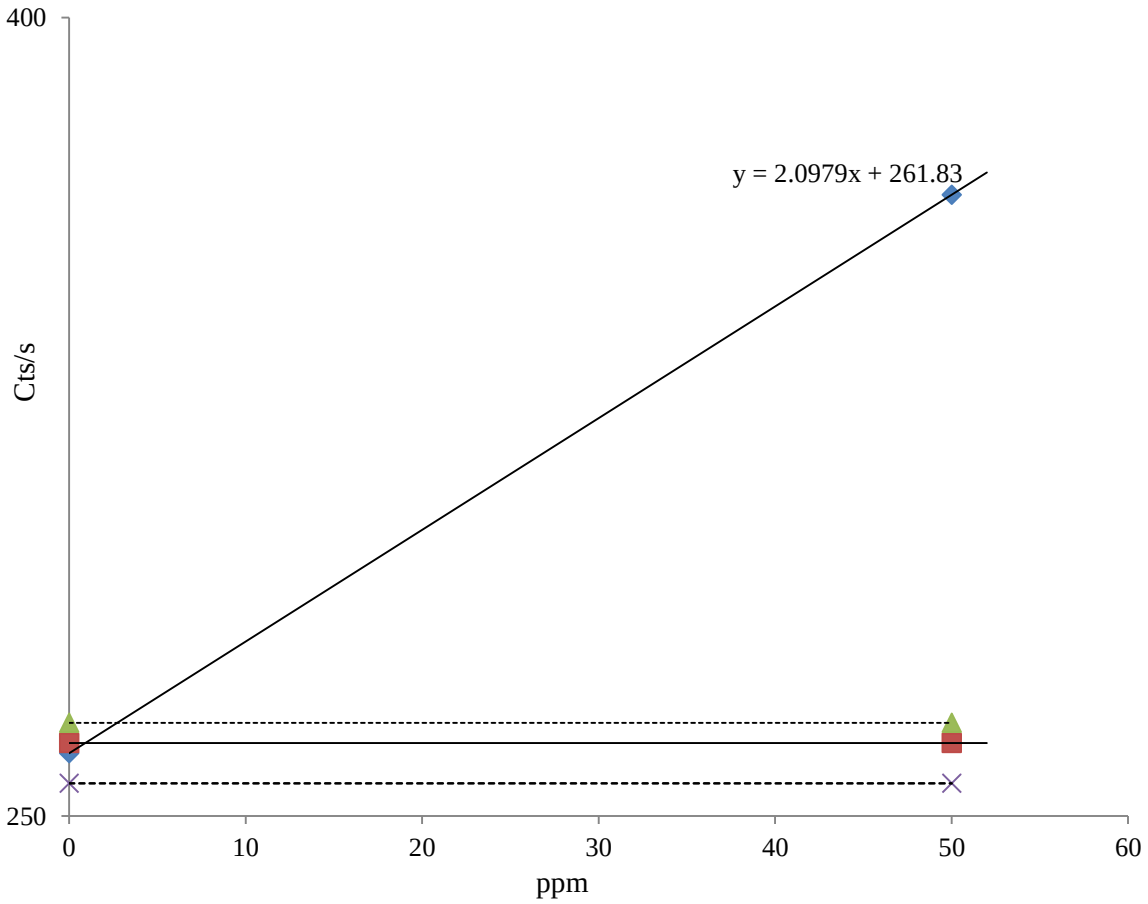

Figure 2: Determination of detection limit of Sb(V) on ICP-OES

Appendix 2.

Calculation of Sb(V) on HAP

$$\frac{Sb(V)}{nm^2} = \frac{X\ mole\ of\ Sb(V)}{g\ (HAP)} * \frac{1g\ (HAP) * 1m^2}{1\ mole * 70.1m^2} * \frac{6.02 * 10^{23}}{10^{18} nm^2}$$